ANTIOXIDANTS & REDOX SIGNALING
Volume 8, Numbers 7 & 8, 2006

Forum Original Research Communication

Mn-Superoxide Dismutase Overexpression Enhances G_2 Accumulation and Radioresistance in Human Oral Squamous Carcinoma Cells

AMANDA L. KALEN, EHAB H. SARSOUR,
SUJATHA VENKATARAMAN, and PRABHAT C. GOSWAMI

ABSTRACT

This study investigates the hypothesis that Mn-superoxide dismutase (MnSOD) influences cancer cell radiosensitivity by regulating the G_2-checkpoint pathway. Human oral squamous carcinoma cells (SCC25) stably overexpressing MnSOD were irradiated (6 Gy) and assayed for cell survival, cell-cycle phase distributions, and bromodeoxyuridine (BrdU) pulse-chase flow-cytometric measurements of cell-cycle phase transits. Electron paramagnetic resonance (EPR) spectroscopy was used to measure steady-state levels of oxygen-centered free radicals. Glutathione and glutathione disulfide levels were used as indicators of changes in the intracellular redox state. MnSOD overexpression increased radioresistance threefold to fourfold; this increase was associated with twofold to threefold increases in radiation-induced G_2 accumulation. BrdU pulse-chase and flow-cytometric measurements of the percentage of G_1 and relative movement showed no significant changes in G_1 and S transits; however, the percentage of G_2 cells and BrdU-positive cells showed delayed G_2+M transits in MnSOD-overexpressing irradiated cells. The steady-state levels of oxygen-centered free radicals were not significantly different in vector compared with MnSOD-overexpressing cells, suggesting that the free radical generation is essentially similar. MnSOD overexpression did prevent radiation-induced decreases in total glutathione content, which correlated with radioresistance and enhanced G_2 accumulation. These results support the hypothesis that a "metabolic redox-response" to IR exposure regulates radiosensitivity by altering radiation-induced G_2 accumulation. *Antioxid. Redox Signal.* 8, 1273–1281.

INTRODUCTION

Mn-superoxide dismutase (MnSOD) is a nuclear-encoded mitochondria-localized metalloenzyme that catalyzes the dismutation of superoxide ($O_2^{\bullet -}$) to hydrogen peroxide (H_2O_2) and oxygen (13). The human MnSOD gene is located on chromosome 6 (6q25), and MnSOD protein exists as a homotetramer (8). In mammalian cells, two other SOD enzymes are found: cytosolic and nuclear copper-zinc SOD, and extracellular SOD. MnSOD knockout mice died within the first 10 days after birth and showed dilated cardiomyopathy, increased lipid accumulation in liver, and metabolic acidosis (19). In recent years, MnSOD has been categorized as a tumor-suppressor gene because MnSOD overexpression inhibits cellular proliferation in a variety of cancer cells in both *in vitro* and *in vivo* model systems (9, 20, 36). Furthermore, ectopic expression of MnSOD rendered cells resistant to the cytotoxic effects of tumor necrosis factor, irradiation, doxorubicin (Adriamycin), and radiation-induced neoplastic transformation (11, 15, 33, 36, 37). The observations that irradiation generates reactive oxygen species (ROS) and fluctuations in ROS levels are believed to influence changes in cellular reduction and oxidation (redox) state, it is hypothesized that MnSOD-induced changes in cancer cell radiation sensitivity could be regulated by alterations in cellular redox state.

Free Radical and Radiation Biology Program, Department of Radiation Oncology, University of Iowa, Iowa City, Iowa.

The potential for ROS signaling regulating cellular processes after oxidative stress has recently gained significant attention (6, 7, 12, 18). Cellular responses to ionizing radiation depend on both cell-cycle positions at the time of irradiation and activation of cell-cycle checkpoint pathways. It is well known that cells in the G_2 and M phases are highly radiosensitive; late S-phase cells are most radioresistant, with G_1 cells having an intermediate response (34). Cancer cell radiosensitivity is also influenced by radiation-induced activation of cell-cycle checkpoint pathways, primarily in G_1 and G_2. Cell-cycle checkpoints prevent DNA replication and cellular division in cells with damaged macromolecules (16, 21). The G_1 checkpoint is defective in many cancer cells, primarily due to inactivation of the tumor-suppressor p53 protein (17). However, all cancer cells, irrespective of p53 status, exhibit a radiation-induced G_2 delay (3, 22). Several studies, including the pioneering work of Tolmach, Little, Schneiderman, and Dewey, demonstrate that the radiation-induced G_2 delay is dose dependent, and the duration of this delay, in general, correlates with radiosensitivity (10, 23, 26, 31, 34). Although the quantitative significance of the intracellular redox environment in radiosensitivity is not fully understood, we have previously shown that manipulations of the intracellular redox state influence cell-cycle progression and cell-cycle regulatory protein levels (24, 25, 28). Therefore, it is reasonable to postulate that MnSOD activity influences the intracellular redox state in irradiated cells, which then regulates cell-cycle checkpoint activation and radiosensitivity of cancer cells.

MATERIALS AND METHODS

Cell culture and MnSOD activity assay

The human oral squamous carcinoma wild-type, vector control, and MnSOD overexpressing SCC-25 cells were generous gifts from Dr. Larry W. Oberley, University of Iowa, Iowa City. The detailed methods of transfecting cells with plasmid DNA containing cytomegalovirus promoter–driven human MnSOD cDNA and selection of stable cell lines were previously published by Liu *et al*. (20). Cells were cultured in DMEM-Ham's F-12, 10% fetal bovine serum (HyClone, Salt Lake City, UT), 0.4 μg/ml hydrocortisone, 0.4 mg/ml Geneticin (G418), and antibiotics (penicillin and streptomycin) in a 37°C humidified incubator with 5% CO_2 and 95% air. MnSOD protein levels and enzymatic activities were verified by immunoblotting and native-activity gel electrophoresis analysis, following the methods of Darby *et al*. (9). Exponentially growing asynchronous cultures were harvested by scraping, and cell pellets were stored at −20°C. The pellets were resuspended in phosphate-buffered saline and sonicated. One hundred micrograms of total cellular protein was separated on a 12% native polyacrylamide gel electrophoresis. After electrophoresis, the gel was soaked in a solution containing 2.43 m*M* nitroblue tetrazolium (NBT), 28 μ*M* riboflavin, and 28 m*M* TEMED for 20 min in the dark. The gel was rinsed with distilled water and illuminated under a fluorescent lamp for visualization of MnSOD activity. The bands were visualized and quantified with a computerized digital imaging system interfaced with AlphaImager 2000 software (Alpha Innotech, San Leandro, CA).

Ionizing radiation

The University of Iowa Holden Comprehensive Cancer Center Radiation and Free Radical Core facility resources were used for all radiation-related experiments. Exponentially growing asynchronous cultures were irradiated by using a cesium-137 gamma radiation source set at a dose rate of 0.84 Gy/min.

Cell-survival assays

Monolayer cultures of exponential control and irradiated cells were trypsinized, and appropriate dilutions of cell cultures were replated for colony-formation assay. Cells were cultured for 12–14 days and stained with 0.005% crystal violet in 70% ethanol. Colonies of ≥50 cells were counted. Plating efficiencies for all treatments were used for clonogenic survival corrections.

In a separate series of experiments, control and irradiated monolayer cultures were continued in culture, and cell viability was assayed by propidium iodide (PI) dye exclusion and flow-cytometry assay. Cells resuspended in cold phosphate-buffered saline were incubated with PI (1 μg/ml) and fluorescence assayed by flow cytometry. Fluorescence from 10,000 cells was collected in list mode, and populations of PI-positive (nonviable) and PI-negative (viable) cells were calculated by using WINMDI software.

Flow-cytometry assays for measurements of cell cycle–phase distributions

Cell cycle–phase distributions were analyzed by both PI staining of ethanol-fixed cells and a bromodeoxyuridine (BrdU) pulse-chase bivariate flow-cytometry assay (see later). Ethanol-fixed cells were treated with RNase A (0.1 mg/ml) for 30 min followed by incubation with PI (35 μg/ml). DNA content of PI-stained cells was analyzed by FACScan (Becton Dickinson, Franklin Lakes, NJ), and fractions of cells in G_1, S, and G_2+M were calculated by using CellQuest Pro (Becton Dickinson) and MODFIT software (Verity Software House, Topsham, ME).

BrdU pulse-chase dual-parameter flow-cytometry assay was performed by following our previously published protocols (24, 25, 28). The assay is designed for simultaneous measurement of transits through G_1, S, and G_2+M cell-cycle phase in both parental and daughter generations. In brief, unirradiated and irradiated asynchronous cultures were pulse-labeled with BrdU for 30 min immediately after irradiation. Cells were continued in culture in BrdU-free growth medium and harvested by trypsinization at various hours after irradiation. Ethanol-fixed cells were stored at 4°C before flow-cytometry assay. Nuclei were isolated from ethanol-fixed cells and incubated with anti-BrdU primary antibody followed by incubation with fluorescein isothiocyanate (FITC)-conjugated goat anti-mouse secondary antibody (Becton Dickinson). The nuclei were treated with RNase A for 30 min and stained with PI. FITC and PI fluorescence of 20,000 nuclei were collected in list mode and analyzed by

using CellQuestPro and WINMDI software. Transits through different cell-cycle phases were calculated as follows: Fig. 3: (a) G_1 transit is the number of nuclei (events) in box 1/total number of events; (b) G_2 transit is the number of events in box 2/total number of events; (c) S transit is the measurements of relative movement (RM, ref. 2), RM = [(Mean channel number of events in box 3 – mean channel number of events in box 1)/(Mean channel number of events in box 2 – mean channel number of events in box 1)]; (d) transit through S, G_2, and M phases (fraction G_1^+) = (Number of events in box 4/2)/[(Number of events in box 3) + (Number of events in box 4/2)]. Events marked G_1^+ (box 4) represent BrdU-positive cells transiting through S, G_2, and M. All flow-cytometry measurements were performed at the University of Iowa Flow Cytometry Core facility.

Electron paramagnetic resonance (EPR) assay of oxygen-centered radicals

The University of Iowa EPR core facility resources and expertise were used to perform EPR assay. In this method, a diamagnetic compound (spin trap) reacts with short-lived paramagnetic free radicals to form spin adducts, which are detectable by EPR. The spin adducts have a longer half-life compared with the original free radical, allowing them to accumulate to a detectable level. The EPR spectrum of the spin-adduct is unique for the given radical, having characteristic hyperfine splitting (4). Superoxide radical reacts with 5,5-dimethyl-1-pyrroline *N*-oxide (DMPO), initially forming DMPO/OOH. DMPO/OOH is unstable and can be rapidly converted to DMPO/OH (5). Monolayer cultures were rinsed with PBS, irradiated, and layered with PBS containing the chelating resin, iminodiacetic acid and 100 m*M* spin trap DMPO. Cells were transferred to a flat-cell, and EPR spectra of DMPO-OH were recorded by using a Bruker EMX 300 spectrometer with a magnetic field modulation frequency of 100 kHz and microwave power of 40 mW. The scans were traced with modulation amplitude of 1 G, scan rate of 84 s, time constant of 82 s, and receiver gain of 1×10^5. The time from the end of the irradiation and recording of EPR spectra was ~0.5 h. EPR peak heights were calculated by using WinEPR software (Bruker Billerka, MA). Data were first normalized to cell number and fold change calculated relative to unirradiated controls for each cell line.

Measurement of intracellular glutathione levels

Intracellular GSH/GSSG levels were measured by using the resources and expertise provided by the University of Iowa Holden Comprehensive Cancer Center Radiation and Free Radical Core facility. Cell pellets stored frozen at –80°C were homogenized in 50 m*M* potassium phosphate buffer (pH 7.8) containing 1.34 m*M* diethylenetriaminepenta-acetic acid. Total glutathione content was determined in sulfosalicylic acid extracts (5% SSA, wt/vol) by the method of Anderson (1). Reduced (GSH) and oxidized (GSSG) glutathione were distinguished by addition of 2-vinylpyridine, and amounts of individual thiols were normalized per milligram protein in whole-cell extract following previously published methods (24, 30).

Statistical analysis

All results were compared with that of specific controls by using the Student *t* test and analysis of variance (ANOVA) with post hoc test (GraphPad Prism version 4). Homogeneity of variance was assumed with a 95% confidence interval level. Results with p values < 0.05 were considered significant.

RESULTS

MnSOD-overexpressing human oral squamous cancer cells are radioresistant

To determine whether MnSOD regulates radiosensitivity in cancer cells, human oral squamous cancer cells (SCC-25, mutant p53 phenotype) stably overexpressing MnSOD (20) were irradiated with 6 Gy of ionizing radiation (dose rate, 0.84 Gy/min), and assayed for cell survival by both colony-forming assay and a flow cytometry–based PI staining of nonfixed cells. Initial experiments were performed to measure MnSOD protein and enzyme activity levels in unirradiated vector control (V) and MnSOD-overexpressing cells. Consistent with previously published results (20), MnSOD activity levels were higher in MnSOD-overexpressing cells compared with vector control (data not shown). Results from the PI viability assay showed that >40% of the vector control cells were PI positive (nonviable) 4 days after irradiation compared with ~15–25% PI-positive cells in MnSOD-overexpressing cells (Fig. 1A and B; $p < 0.05$). Increased radioresistance in MnSOD-overexpressing cells was also apparent from results obtained from the clonogenic cell-survival assay (Fig. 1C). MnSOD-overexpressing cells were fourfold to fivefold more radioresistant than wild-type controls ($p < 0.05$). These results demonstrate that MnSOD-overexpressing human oral squamous cancer cells are radioresistant.

MnSOD-induced radioresistance in human oral squamous cancer cells is associated with enhanced G_2 accumulation

To determine whether MnSOD-induced radioresistance is associated with altered cell cycle–checkpoint activation, exponential cultures were irradiated with 6 Gy and harvested 10 h after irradiation. Ethanol-fixed cells were treated with RNase A, stained with PI, and DNA content analyzed with flow cytometry by following our previously published protocols (24, 25, 28). Results presented in Fig. 2A show percentage of G_2 cells in unirradiated vector control (16%), and MnSOD-overexpressing cells (17%) were not significantly different. Consistent with earlier reports in the literature, irradiation caused an increase in the percentage of G_2 cells in both vector control and MnSOD-overexpressing cells at 10 h after irradiation (Fig. 2B). However, the increases in percentage of G_2 cells differ significantly in MnSOD-overexpressing cells (60–70%) compared with vector control (40%; $p < 0.05$). A corresponding decrease was noted in the percentage of G_1 cells in MnSOD-overexpressing cells (4–6%) compared with vector control (14%).

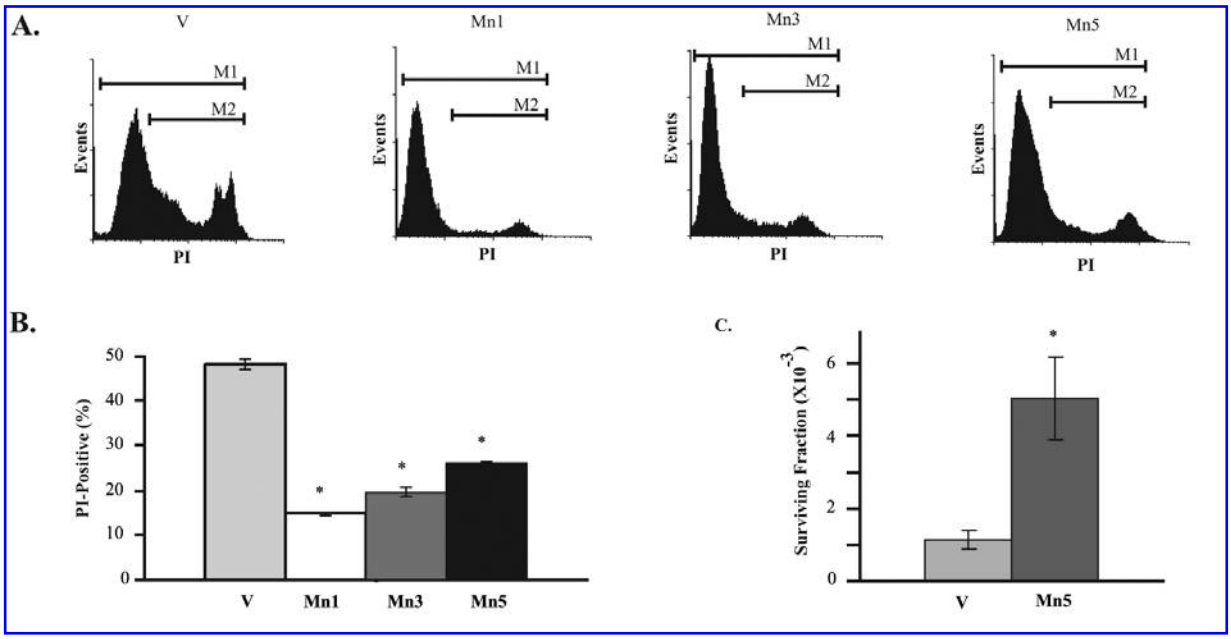

FIG. 1. MnSOD overexpressing human oral squamous carcinoma cells are radioresistant. Exponential cultures of vector control (V) and stably transfected MnSOD overexpressing (Mn1, Mn3 and Mn5) human oral squamous cancer cells (SCC25) were irradiated with 6 Gy (^{137}Cs; 0.84 Gy/min) and continued in culture for an additional 4 days. Both monolayer cells and cells in the media were collected and stained with propidium iodide (PI) prior to flow cytometry assay. Representative histograms are shown on the top panel **(A)**, and quantitation of results is shown in the bottom panel **(B)**; PI-positive cells were scored as nonviable. **(C)** Colony survival assay: appropriate dilutions of irradiated and unirradiated cells were cultured for 12–14 days. Cells were stained with 0.005% crystal violet in 70% ethanol and colonies ≥50 cells counted. Plating efficiencies for all treatments were used for clonogenic survival corrections. Asterisks represent statistical significance ($p < 0.05$); wt: wild type cells; Mn5: MnSOD overexpressing Mn5 clone.

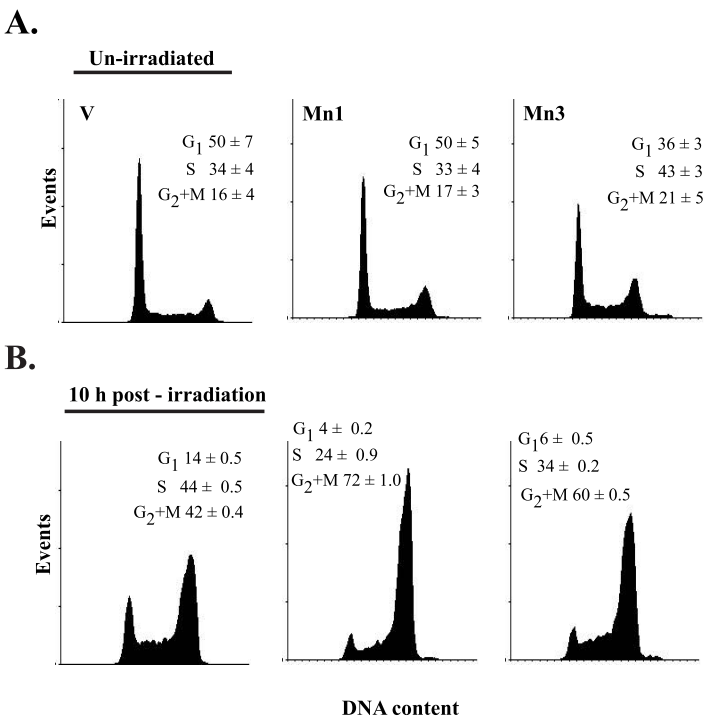

FIG. 2. MnSOD overexpression enhanced G2-accumulation in irradiated human oral squamous cancer cells. Exponentially growing asynchronous cultures were irradiated with 6 Gy. Cells were harvested at the time of irradiation and 10 h postirradiation. Ethanol-fixed cells were treated with RNase A and stained with PI. DNA content assayed by flow cytometry and cell cycle phase distributions calculated using CellQuest and MODFIT software. Representative histograms of unirradiated cells are shown in **(A)** and histograms in **(B)** represent cell cycle phase distributions at 10 h postirradiation (average ± Stdv).

Results from the PI assay do not clearly distinguish the DNA content of late S from G_2, so it was difficult to conclude whether MnSOD overexpression induced a late S-phase checkpoint or a G_2 accumulation in irradiated cells. Therefore, we have designed a BrdU pulse-chase assay to determine simultaneously transits through G_1, S, and G_2+M in control and irradiated cells. Asynchronously growing exponential cultures were irradiated with 6 Gy and pulse-labeled with BrdU for 30 min immediately after irradiation. Cells were continued in culture in BrdU-free medium and harvested at the indicated hours for bivariate flow-cytometry assay. Fractions of G_1, G_2, labeled S-phase cells completing division (G_1^+) and relative movement (RM) were calculated. Results show that transit through G_1 (~14 h) and S (~10 h) in irradiated MnSOD-overexpressing cells was not significantly different compared with irradiated wild-type cells (Fig. 3C and D). Likewise, progression of initial G_2-phase cells to M phase did not appear to differ in irradiated MnSOD-overexpressing cells compared with wild-type cells (Fig. 3E; 0–3 h after irradiation). However, when irradiated S-phase (and possibly G_1) cells reached late S and/or G_2, their exit to M was delayed in MnSOD-overexpressing cells compared with wild-type cells. Furthermore, a larger percentage of G_2 cells were detected in MnSOD-overexpressing irradiated cells relative to wild-type cells. The delay in G_2+M transit in MnSOD over-expressing irradiated cells is also evident from results presented in Fig. 3B. A calculation of the fraction of cells in the G_1^+ compartment (box 4 marked in the right histogram), which represents BrdU-positive S-phase cells that completed cell division, clearly shows irradiated wild-type cells completing cell division ahead of irradiated MnSOD-overexpressing cells (compare number of events in box 4 in wt and Mn5 cells at 24 h after irradiation; Fig. 3B). Twenty-four hours after radiation exposure, ~80% of the BrdU-labeled S-phase cells progressed through S, G_2, and M phases in wild-type cells (Fig. 3B). In contrast, ~40% of S-phase cells in MnSOD-overexpressing cells completed cell division during the same time interval. These results clearly demonstrate that MnSOD overexpression delays irradiated S-phase cell (and possibly G_1 cell) transit through late S and G_2+M phases.

MnSOD-induced radioresistance and enhanced G_2 accumulation correlate with changes in intracellular redox state

To determine whether changes in intracellular redox state could contribute to the radioresistance and enhanced G_2 accumulation in MnSOD-overexpressing cells, an EPR assay was applied to measure the steady-state levels of oxygen-centered radicals immediately after the radiation exposure. Exponentially growing monolayer cultures were rinsed with PBS and irradiated with 6 Gy. Immediately after the radiation exposure, the PBS buffer was replaced with chelated buffer con-

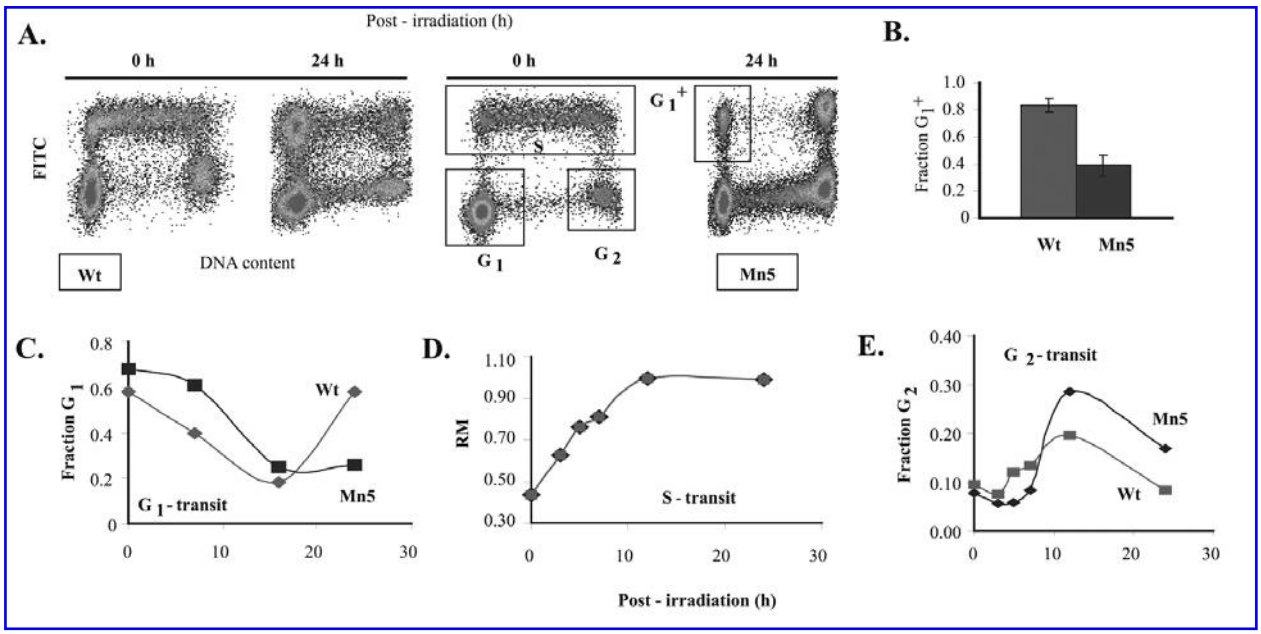

FIG. 3. MnSOD overexpression did not affect transits through G_1 and S in irradiated human oral squamous cells, but a larger fraction of these G_1 and S phase cells accumulate in the G_2-phase. Exponential cultures were pulse-labeled for 30 min with bromodeoxyuridine (BrdU, a thymidine analogue routinely used to label S-phase) immediately after a 6 Gy irradiation, and continued in culture in absence of BrdU. At indicated times, cells were trypsinized and fixed in 70% ethanol. Bivariate flow cytometry assay of DNA content (PI-staining) and FITC-positive nuclei were analyzed following previously published protocol (24, 25, 28). Representative FITC and PI bivariate histograms are shown in panel **A**: left two histograms represent cell cycle phase distributions in wild type cells at the time of radiation and 24 h postirradiation; right two histograms represent MnSOD overexpressing (Mn5) cells. Fraction of BrdU-labeled S-phase cells (G_1^+, box 4) completing cell division is shown in **B**, 24 h postirradiation. Fraction of G_1 (panel **C**, box 1), relative movement (RM; panel **D**), and G_2-fraction (panel **E**, box 2) were calculated from 20,000 nuclei using CellQuest software. A repeat of the experiment showed similar results.

taining DMPO and EPR spectra recorded 30 min later. EPR peak heights were measured, and results were calculated relative to 1 million cells. The fold changes in EPR peak heights were relative to those of unirradiated controls (Fig. 4). These results show that 6-Gy irradiation did not significantly affect the steady-state levels of oxygen-centered free radicals immediately after the radiation exposures.

To determine whether intracellular redox state could differ in irradiated cells long after the beam is turned off and if such a change in redox state differs in MnSOD-overexpressing cells, cells were scrape-harvested at the time of irradiation, 6, 10, and 24 h after irradiation. Changes in GSH and GSSG levels were used as indicators of perturbations in intracellular redox state. These results show that intracellular total glutathione levels were high in vector control cells at the time of irradiation (50 nmol/mg protein), which decreased to 13 nmol/mg protein at 6 h after irradiation and remained low (4–5 nmol/mg protein) at 10 and 24 h after irradiation (Fig. 5A; $p < 0.05$ for all time points compared with 0 h). Interestingly, compared with vector control cells, intracellular total glutathione levels in MnSOD-overexpressing cells (Mn3) were low (24 nmol/mg protein) at the time of irradiation ($p < 0.05$), decreased to 11 nmol/mg protein at 6 h after irradiation ($p < 0.05$ compared with 0 h MnSOD-overexpressing cells), and quickly recovered to normal levels by 10 h after irradiation. In vector control irradiated cells, the percentage of GSSG increased twofold at 10 h after irradiation (8% at the time of irradiation, increasing to 17% at 10 h after irradiation; $p < 0.05$) and returned to normal levels at 24 h after irradiation (Fig. 5B). Percentage of GSSG in MnSOD-overexpressing cells was 3% at the time of irradiation, which increased to 7% at 6 h after irradiation and returned to basal levels at 10 h after irradiation. The percentage of GSSG decreased further at 24 h after irradiation. These results demonstrate that irradiation shifts the intracellular redox state toward a more oxidizing environment in vector control cells, whereas MnSOD overexpression suppresses this increase.

DISCUSSION

ROS are oxygen-containing molecules that have higher chemical reactivity than ground-state molecular oxygen. ROS, including superoxide, hydrogen peroxide, hydroxyl radical, singlet molecular oxygen, and organic hydroperoxides, are constantly generated intracellularly as by-products of aerobic metabolism and have traditionally been thought of as unwanted and toxic products of living in an aerobic environment (12). It is well known that exposure of cells to ionizing radiation (IR) generates ROS that persist for milliseconds and result in oxidative damage to cellular macromolecules. It has been hypothesized that ROS-mediated covalent modifications of cellular macromolecules could regulate some aspects of the cellular responses to IR exposure (32). This assumption was based on the observations that manipulations of antioxidants (antioxidant enzymes and other ROS scavengers) before the IR exposure suppress many of the biologic effects of irradiation. Therefore, maintenance of a redox balance (production of ROS and their removal) appears to have a mechanistic function regulating many of the cellular processes.

Reports from other laboratories and our recent observations of intracellular redox state regulating cell-cycle progression support the hypothesis that ROS can serve as second messengers regulating redox-sensitive cell-cycle regulatory processes during cellular proliferation (12, 14, 24, 25, 28). Although hydrogen peroxide could influence the redox state of protein thiols (cysteines; -SH, reduced to –S-S-, oxidized), superoxide could alter the redox state of metal cofactors (*e.g.*,

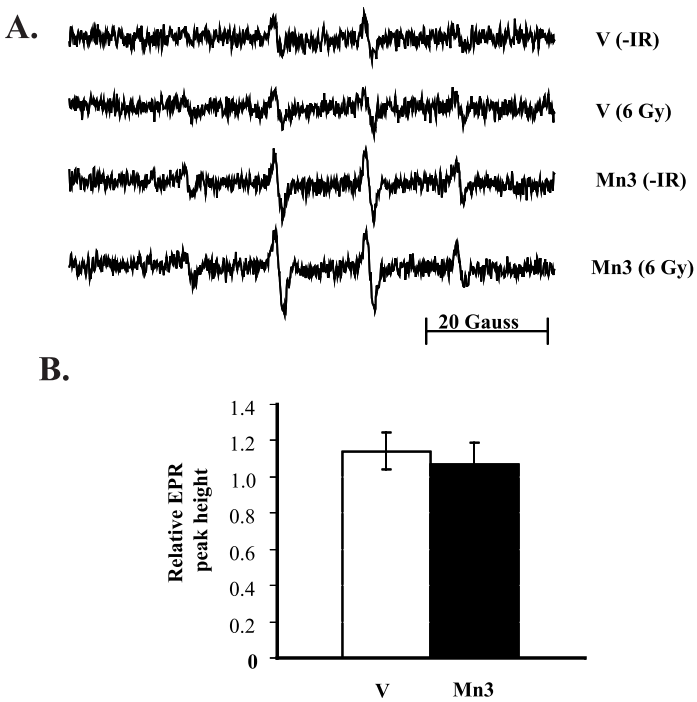

FIG. 4. Irradiation does not alter the steady state levels of oxygen-centered radicals immediately after the radiation exposure in MnSOD overexpressing cells compared to vector control. Asynchronously growing monolayer cultures of vector control (V) and MnSOD overexpressing (Mn3) cells were rinsed with chelated PBS, and layered with 500 μl of chelated PBS buffer containing 100 m*M* of the spin trap, DMPO. Cells were scraped and transferred immediately to a flat cell for EPR measurements. EPR spectra of DMPO-OH were recorded using a Bruker EMX-300 series spectrometer. **(A)** Representative EPR spectra for unirradiated and 6 Gy irradiated cells; **(B)** EPR peak heights per one million cells were determined using WinEPR software. Fold change was calculated as the ratio of peak height for the irradiated cells to that of the corresponding unirradiated cells.

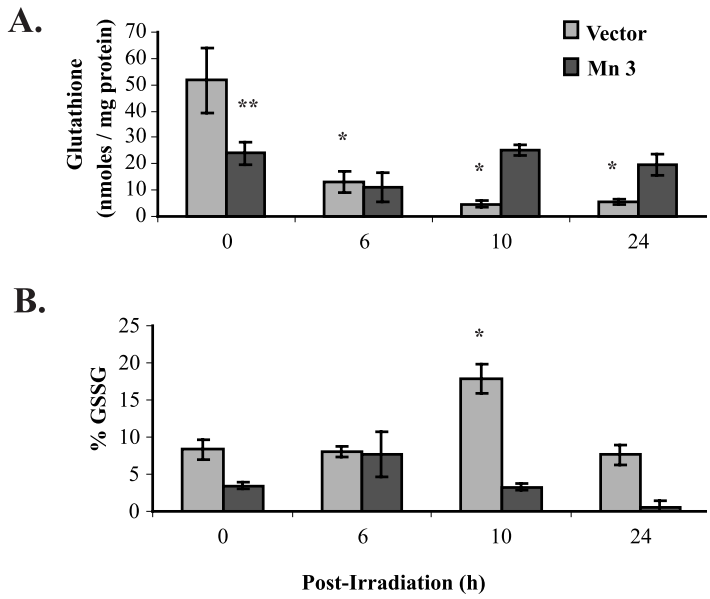

FIG. 5. MnSOD overexpression appears to suppress radiation-induced changes in intracellular redox state. Asynchronously growing exponential cultures were irradiated with 6 Gy and cells were scrape-harvested at the time of irradiation (0 h), 6, 10, and 24 h postirradiation. Intracellular GSH/GSSG levels were measured using a spectrophotometric assay. The assay was performed using resources and expertise provided by the University of Iowa Holden Comprehensive Cancer Center Radiation and Free Radical Core facility. Asterisks represent statistical significance in irradiated vector cells compared to 0 h; double asterisks represent statistical significance of unirradiated MnSOD overexpressing cells compared to unirradiated vector control. Statistical analysis was done using GraphPad Prism version 4 software.

Fe and Cu) present in many kinases and phosphatases. Thus, the potential for ROS (mitochondria, cytosolic, or both) to mediate cell signaling after oxidative stress has recently gained significant attention. Although the majority of these research endeavors focus on cell death, in particular apoptosis, we have previously shown that progression through the cell cycle is a redox-sensitive process (14, 24, 25, 28). With this finding, we hypothesize that radiation, which is known to generate ROS, activates cell-cycle checkpoints through redox-sensitive signaling pathways.

IR exposure is known to cause cell-cycle arrest in G_1, S, and/or G_2 to prevent replication on damaged DNA or to prevent aberrant cell division. The regulatory mechanisms are known as checkpoints, and their primary function is to delay progression until the cell has adequately repaired the damage. Because the G_1 checkpoint is defective in many cancer cells, primarily due to inactivation of the tumor-suppressor p53 protein (17), cancer cells depend on the G_2 checkpoint for survival. This property makes cancer cells susceptible to therapies targeted at abrogating the G_2 delay; not surprisingly, numerous research efforts are aimed at a better understanding of the mechanisms regulating the G_2 checkpoint. Our results show that MnSOD overexpression induces radioresistance in human oral squamous cancer cells (Figs. 1–3). Because MnSOD is a mitochondrial localized protein and dismutates superoxide to hydrogen peroxide, these results suggest that mitochondrial metabolism in response to IR exposure could be a significant determinant of cancer cell radiosensitivity. MnSOD-induced radioresistance correlates with an increase in the fraction of G_2 cells and delayed progression through G_2+M (Figs. 2 and 3). These results are consistent with our hypothesis that intracellular redox state could play a significant role regulating progression through specific cell-cycle phases in response to IR exposure.

IR-induced G_2 delay consists of the activation of the G_2 checkpoint (initial G_2 cells transiting to M) and G_2 accumulation (G_1 and S cells accumulating in G_2). IR-induced G_2 checkpoint occurs within hours (~45 min to 1 h) of irradiation, whereas G_2 accumulation manifests several hours after the IR exposure (34). Results from Fig. 3E (0–3 h after irradiation) suggest that MnSOD overexpression (and therefore mitochondrial redox metabolism) might not affect IR-induced G_2-checkpoint activation in human oral squamous cancer cells because exit of cells from G_2 during 3-h post-IR appeared to be similar in control and MnSOD-overexpressing cells. In contrast, mitochondrial metabolism subsequent to the IR exposure could regulate IR-induced G_2 accumulation because the percentage of G_2 increased significantly in MnSOD-overexpressing cells compared with control (Fig. 3E). MnSOD overexpression–induced increase in G_2 accumulation could result in radioresistance because the duration of G_2 delay has been shown to correlate directly with radiosensitivity (26, 34). Our results do not show any significant difference in transits through G_1 and S in irradiated MnSOD-overexpressing cells compared with control. However, because the acid denaturation step in the BrdU assay destroys cells in M phase, we cannot rule out the possibility that MnSOD overexpression could affect transit through M phase in irradiated cells.

The concept of intracellular redox-state regulating cell-cycle checkpoint activation is further supported by the results presented in Figs. 4 and 5. Measurement of the steady-state levels of prooxidants (presumably superoxide) by EPR immediately after the radiation exposure did show a minimal increase in both vector control and MnSOD-overexpressing cells. However, the fold change relative to the steady-state levels of prooxidants in unirradiated cells did not show any significant difference in MnSOD-overexpressing cells compared with vector control (Fig. 4). These results indicate that IR-induced generations of free radicals immediately after the IR exposure are essentially similar both in vector control and in MnSOD-overexpressing cells.

However, subsequent scavenging of these free radicals could differ, depending on the antioxidant capacity of the

cell, and it is this "metabolic redox response" to IR exposure that could determine the fate of the redox-sensitive cellular processes in irradiated cells. This hypothesis is supported by earlier reports demonstrating IR-induced increases in pentose cycle activity (35). This increase in pentose cycle activity is thought to provide increased NADPH, which is required for repair and biosynthetic processes. Consistent with these earlier observations of IR-induced changes in cellular metabolic activities, results presented in Fig. 5 showed that IR exposure decreased intracellular GSH levels in both vector control and MnSOD-overexpressing cells at 6 h after irradiation. Although GSH levels continued to decrease at 10 and 24 h after irradiation in vector control cells, GSH levels in irradiated MnSOD-overexpressing cells returned to basal levels by 10 h after irradiation. The initial decrease in GSH levels at 6 h after irradiation precedes IR-induced G_2 delay, suggesting that the IR-induced shift in intracellular redox state to an oxidizing environment could activate the G_2-checkpoint pathway. Although the maintenance of the prooxidant environment in vector control cells at 10 and 24 h after irradiation would facilitate transits through G_2+M, a reducing environment would prolong G_2+M transits in MnSOD-overexpressing cells. This assumption is consistent with results presented in Figs. 2, 3, and 5. These results are also consistent with our earlier observations in which we showed that progression through late S and G_2+M is associated with an increase in intracellular oxidation state (14). In this previous work, we used HeLa cells synchronized by mitotic shake-off and showed that the oxidation of a prooxidant-sensitive probe DCFH-DA was maximal in late S and G_2+M cells compared with G_1 and early S. These results suggest that a more-oxidizing environment favors progression through late S and G_2+M. In a separate study, we showed that a shift in intracellular redox state toward a more reducing environment induces cell-cycle delays (24). Therefore, although a shift in redox state toward an oxidizing environment would initiate the G_2 checkpoint in irradiated cells, a shift toward a reducing environment would sustain the G_2 delay until metabolic processes reestablish communications with the cell-cycle regulatory processes initiating the restart of the stalled cell cycle.

In summary, our results show that MnSOD-induced radioresistance in human oral squamous cancer cells correlates with enhanced G_2 accumulation. These results support the hypothesis that biochemical redox reactions (cellular metabolism) long after the radiation insult could significantly affect the biologic responses to IR exposure. Earlier work of Petkau *et al*. (27) showed that administration of CuZnSOD 2–4 h after the IR exposure protected Swiss mice from radiation-induced lethality. These results suggest that superoxide generated long after the beam is turned off could affect the biologic consequences of the IR exposure. Although speculative, it is possible that superoxide (or hydrogen peroxide) generated from an IR-induced shift in cellular metabolism could serve as second messengers, leading to cell cycle–checkpoint activation, which then regulates radiosensitivity. Therefore, a better understanding of the "metabolic redox response" to IR exposure could provide a biochemical rationale for novel cancer-therapy modalities targeted at cell-cycle checkpoints and antioxidant enzyme pathways.

ABBREVIATIONS

BrdU, bromodeoxyuridine; EPR, electron paramagnetic resonance; FITC, fluorescein isothiocyanate; GSH, glutathione; GSSG, glutathione disulfide; PI, propidium iodide; MnSOD, manganese superoxide dismutase; redox, reduction and oxidation reactions; ROS, reactive oxygen species.

ACKNOWLEDGMENTS

We thank Dr. Larry W. Oberley for the cell lines, Ms. Kelly Andringa and Dr. Douglas R. Spitz for helping with the spectrophotometric assay of thiols, and Dr. Garry Buettner for helping with the EPR assay. NIH RO1 CA111365 and the University of Iowa Carver Research Foundation grants to P.C.G. and PO1CA066081 to L.W.O. supported this work.

REFERENCES

1. Anderson ME. Tissue glutathione. In: Greenwald RA (Ed). *Handbook of Methods for Oxygen Radical Research.* Boca Raton, FL: CRC Press, pp 317–323, 1985.
2. Begg AC, McNally NJ, Shrieve DC, and Karcher H. A method to measure the duration of DNA synthesis and the potential doubling time from a single sample. *Cytometry* 6: 620–626, 1985.
3. Bernhard EJ, Maity A, Muschel RJ, and McKenna WG. Effects of ionizing radiation on cell cycle progression: A review. *Radiat Environ Biophys* 34: 79–83, 1995.
4. Buettner GR. Spin trapping: ESR parameters of spin adducts. *Free Radic Biol Med* 3: 259–303, 1987.
5. Buettner GR. The spin trapping of superoxide and hydroxyl free radicals with DMPO (5–5-dimethylpyrroline-*N*-oxide): More about iron. *Free Radic Res Comm* 19: S79–S87, 1993.
6. Cai J and Jones DP. Superoxide in apoptosis: mitochondrial generation triggered by cytochrome *c* loss. *J Biol Chem* 273:11401–11404, 1998.
7. Chandel NS and Schumacker PT. Cells depleted of mitochondria DNA (rho0) yield insight into physiological mechanisms. *FEBS Lett* 454:173–176, 1999.
8. Church SL, Grant JW, Ridnour LA, Oberley LW, Swanson PE, Meltzer PS, and Trent JM. Increased manganese dismutase expression suppresses the malignant phenotype of human melanoma cells. *Proc Natl Acad Sci U S A* 90: 3113–3117, 1993.
9. Darby Weydert CJ, Smith BB, Xu L, Kregel KC, Ritchie JM, Davis CS, and Oberley LW. Inhibition of oral cancer cell growth by adenovirus *MnSOD* plus BCNU treatment. *Free Radic Biol Med* 34: 316–329, 2003.
10. Dewey WC and Highfield DP. G2 block in Chinese hamster cells induced by X-irradiation, hyperthermia, cycloheximide, or actinomycin D. *Radiat Res* 65: 511–528, 1976.
11. Epperly MW, Defilippi S, Sikora C, Gretton J, Kalend A, and Greenberger JS. Intratracheal injection of manganese superoxide dismutase (MnSOD) plasmid/liposomes pro-

tects normal lung but not orthotopic tumors from irradiation. *Gene Ther* 7: 1011–1018, 2000.
12. Finkel T. Oxygen radicals and signaling. *Curr Opin Cell Biol* 10: 248–253, 1998.
13. Fridovich I. Superoxide dismutases, an adaptation to a paramagnetic gas. *J Biol Chem* 264: 7761–7764, 1989.
14. Goswami PC, Sheren J, Albee LD, Parsian A, Sim JE, Ridnour LA, Higashikubo R, Gius D, Hunt CR, and Spitz DR. Cell cycle-coupled variation in topoisomerase IIalpha mRNA is regulated by the 3′-untranslated region: Possible role of redox-sensitive protein binding in mRNA accumulation. *J Biol Chem* 275: 38384–38392, 2000.
15. Guo G, Sanders YS, Lyn-Cook BD, Wang T, Tamae D, Ogi J, Khaletsky A, Li Z, Weydert C, Longmate JA, Huang TT, Spitz DR, Oberley LW and Li JJ. Manganese superoxide dismutase-mediated gene expression in radiation-induced adaptive responses. *Mol Cell Biol* 23: 2362–2378, 2003.
16. Hartwell L. Defects in a cell cycle checkpoint may be responsible for the genomic instability of cancer cells. *Cell* 71: 543–546, 1992.
17. Hussain SP and Harris CC. p53 mutation spectrum and load: The generation of hypothesis linking the exposure of endogenous or exogenous carcinogens to human cancer. *Mutat Res* 428: 23–32, 1999.
18. Lee HC and Wei YH. Mitochondrial role in life and death of the cell. *J Biomed Sci* 7:2–15, 2000.
19. Li Y, Huang TT, Carlson EJ, Melov S, Ursell PC, Olson JL, Noble LJ, Yoshimura MP, Berger C, Chan PH, Wallace DC, and Epstein CJ. Dilated cardiomyopathy and neonatal lethality in mutant mice lacking manganese superoxide dismutase. *Nat Gen* 11: 376–381, 1995.
20. Liu R, Oberley TD, and Oberley LW. Transfection and expression of MnSOD cDNA decreases tumor malignancy of human oral squamous carcinoma SCC-25 cells. *Hum Gene Ther* 8: 585–595, 1997.
21. O'Connor PM. Mammalian G1 and G2 phase checkpoints. *Cancer Surv* 29: 51–182, 1997.
22. Maity A, Kao GD, Muschel RJ, and McKenna WG. Potential molecular targets for manipulating the radiation response. *Int J Radiat Oncol Biol Phys* 37: 639–653, 1997.
23. McKeena WG, Illiakis G, Weiss MC, and Muschel RJ. Increased G2 delay in radiation-resistant cells obtained by transformation of primary rat embryo cells with the oncogenes H-ras and V-myc. *Radiat Res* 125: 283–287, 1991.
24. Menon SG, Sarsour EH, Spitz DR, Higashikubo R, Sturm M, Zhang H, and Goswami PC. Redox regulation of the G1 to S phase transition in the mouse embryo fibroblast cell cycle. *Cancer Res* 63: 2109–2117, 2003.
25. Menon SG, Coleman MC, Walsh SA, Spitz DR, and Goswami PC. Differential susceptibility of nonmalignant human breast epithelial cells and breast cancer cells to thiol antioxidant-induced G1-delay. *Antioxid Redox Signal* 7: 711–718, 2005.
26. Nagasawa H, Keng P, Harley R, Dahlberg W, and Little JB. Relationship between gamma-ray-induced G2/M delay and cellular radiosensitivity. *Int J Radiat Biol* 66: 373 –379, 1994.
27. Petkau A, Chelack WS, and Pleskach SD. Protection of post-irradiated mice by superoxide dismutase. *Int J Radiat Biol* 29: 297–299, 1976.
28. Sarsour EH, Agarwal M, Pandita TK, Oberley LW, and Goswami PC. Manganese superoxide dismutase protects the proliferative capacity of confluent normal human fibroblasts. *J Biol Chem* 280: 18033–18041, 2005.
29. Su L and Little JB. Prolonged cell cycle delay in radio-resistant human cell lines transfected with activated *ras* oncogene and/or simian virus 40 T-antigen. *Radiat Res* 133: 73–79, 1993.
30. Ridnour LA, Winters RA, Ercal N, and Spitz DR. Measurement of glutathione, glutathione disulfide, and other thiols in mammalian cell and tissue homogenates using high-performance liquid chromatography separation of *N*-(1-pyrenyl) maleimide derivatives. *Methods Enzymol* 299: 258–267, 1999.
31. Schneiderman MH, Dewey WC, Leeper DB, and Nagasawa H. Use of the mitotic selection procedure for cell cycle analysis. *Exp Cell Res* 74: 430–438, 1972.
32. Spitz DR, Azzam EI, Li JJ, and Gius D. Metabolic oxidation/reduction reactions and cellular responses to ionizing radiation: A unifying concept in stress response biology. *Cancer Metastasis Rev* 23: 311–322, 2004.
33. Takada Y, Hachiya M, Park SH, Osawa Y, Ozawa T, and Akashi M. Role of reactive oxygen species in cells overexpressing manganese superoxide dismutase: Mechanism for induction of radioresistance. *Mol Cancer Res* 1: 137–146, 2002.
34. Terasima T and Tolmach LJ. Variations in several responses of HeLa cells to X-irradiation during the division cycle. *Biophys J* 3: 11–33, 1963.
35. Tuttle SW, Varnes ME, Mitchell JB, and Biaglow JE. Sensitivity to chemical oxidants and radiation in CHO cell lines deficient in oxidative pentose cycle activity. *Int J Radiat Oncol Biol Phys* 22: 671–675, 1992.
36. Venkataraman S, Jiang X, Weydert C, Zhang Y, Zhang HJ, Goswami PC, Ritchie JM, Oberley LW, and Buettner GR. Manganese superoxide dismutase overexpression inhibits the growth of androgen-independent prostate cancer cells. *Oncogene* 24: 77–89, 2005.
37. Wong GHW, Elwell JH, Oberley LW, and Goeddel DV. Manganese superoxide dismutase is essential for cellular resistance to cytotoxicity of tumor necrosis factor. *Cell* 58: 923–931, 1989.
38. Yen SC, Oberley TD, Vichitbandha S, Ho YS, and St. Clair DK. The protective role of manganese superoxide dismutase against Adriamycin-induced acute cardiac toxicity in transgenic mice. *J Clin Invest* 98: 1253–1260, 1996.

Address reprint requests to:
Prabhat C. Goswami, Ph.D.
Free Radical and Radiation Biology Program
Department of Radiation Oncology
B180 Medical Laboratories
University of Iowa
Iowa City, IA 52242

E-mail: prabhat-goswami@uiowa.edu

Date of first submission to ARS Central, January 13, 2006; date of acceptance, February 1, 2006.

This article has been cited by:

1. Maneesh G. Kumar, Neil M. Patel, Adam M. Nicholson, Amanda L. Kalen, Ehab H. Sarsour, Prabhat C. Goswami. 2012. Reactive oxygen species mediate microRNA-302 regulation of AT-rich interacting domain 4a and C-C motif ligand 5 expression during transitions between quiescence and proliferation. *Free Radical Biology and Medicine* **53**:4, 974-982. [CrossRef]
2. Fanny Caputo, Rolando Vegliante, Lina Ghibelli. 2012. Redox modulation of the DNA damage response. *Biochemical Pharmacology* . [CrossRef]
3. Isabel Quiros-Gonzalez, Rosa M. Sainz, David Hevia, Juan C. Mayo. 2011. MnSOD drives neuroendocrine differentiation, androgen independence, and cell survival in prostate cancer cells. *Free Radical Biology and Medicine* **50**:4, 525-536. [CrossRef]
4. Ting-Ying Fu, Yu-Yi Hou, Sau-Tung Chu, Ching-Feng Liu, Cheng-Hui Huang, Hung-Chih Chen, Michael Hsiao, Pei-Jung Lu, Jyh-Seng Wang, Luo-Ping Ger. 2011. Manganese superoxide dismutase and glutathione peroxidase as prognostic markers in patients with buccal mucosal squamous cell carcinomas. *Head & Neck* n/a-n/a. [CrossRef]
5. Chien-Yu Lin, Hung-Ming Wang, Chung-Jan Kang, Li-Yu Lee, Shiang-Fu Huang, Kang-Hsing Fan, Eric Yen-Chao Chen, I-How Chen, Chun-Ta Liao, Joseph Tung-Chieh Chang. 2010. Primary Tumor Site as a Predictor of Treatment Outcome for Definitive Radiotherapy of Advanced-Stage Oral Cavity Cancers. *International Journal of Radiation Oncology*Biology*Physics* **78**:4, 1011-1019. [CrossRef]
6. Aaron K. Holley, Yong Xu, Daret K. St. Clair, William H. St. Clair. 2010. RelB regulates manganese superoxide dismutase gene and resistance to ionizing radiation of prostate cancer cells. *Annals of the New York Academy of Sciences* **1201**:1, 129-136. [CrossRef]
7. Ehab H. Sarsour , Maneesh G. Kumar , Leena Chaudhuri , Amanda L. Kalen , Prabhat C. Goswami . 2009. Redox Control of the Cell Cycle in Health and Disease. *Antioxidants & Redox Signaling* **11**:12, 2985-3011. [Abstract] [Full Text HTML] [Full Text PDF] [Full Text PDF with Links]
8. Hidetaka Yokoe, Hitomi Nomura, Yukio Yamano, Kazuaki Fushimi, Yosuke Sakamoto, Katsunori Ogawara, Masashi Shiiba, Hiroki Bukawa, Katsuhiro Uzawa, Yuichi Takiguchi, Hideki Tanzawa. 2009. Characterization of intracellular superoxide dismutase alterations in premalignant and malignant lesions of the oral cavity: correlation with lymph node metastasis. *Journal of Cancer Research and Clinical Oncology* **135**:11, 1625-1633. [CrossRef]
9. Zhen Gao, Ehab H. Sarsour, Amanda L. Kalen, Ling Li, Maneesh G. Kumar, Prabhat C. Goswami. 2008. Late ROS accumulation and radiosensitivity in SOD1-overexpressing human glioma cells. *Free Radical Biology and Medicine* **45**:11, 1501-1509. [CrossRef]
10. Venkatasubbaiah A. Venkatesha, Sujatha Venkataraman, Ehab H. Sarsour, Amanda L. Kalen, Garry R. Buettner, Larry W. Robertson, Hans-Joachim Lehmler, Prabhat C. Goswami. 2008. Catalase ameliorates polychlorinated biphenyl-induced cytotoxicity in nonmalignant human breast epithelial cells. *Free Radical Biology and Medicine* **45**:8, 1094-1102. [CrossRef]
11. Ehab H. Sarsour, Sujatha Venkataraman, Amanda L. Kalen, Larry W. Oberley, Prabhat C. Goswami. 2008. Manganese superoxide dismutase activity regulates transitions between quiescent and proliferative growth. *Aging Cell* **7**:3, 405-417. [CrossRef]